## Fully charm tetraquark production at hadronic collisions with gluon radiation effects

Yefan Wang<sup>1,2,\*</sup> and Ruilin Zhu<sup>1,2,†</sup>

We have performed, for the first time, a complete next-to-leading order QCD calculation for processes involving fully charm tetraquark states, revealing that the renormalization constant of the color-singlet four charm quark operator is exactly unity at this order. By resumming over various gluon radiation effects, we have improved the precision of their hadroproduction cross-section to the order of  $\mathcal{O}(\alpha_s^5)$ . Through symmetry analysis, we investigated the possible quark configurations of the fully charm tetraquark and expanded its states in the color symmetry-antisymmetry basis. By combining LHCb data on the total cross section of the exotic hadron X(6900) and CMS measurements of its spin-parity, we extracted the non-perturbative but universal long-distance matrix elements. The rapidity and transverse momentum distributions are also predicted, which await further experimental verification.

Introduction. Charm family hadrons, according to the color confinement principle, are believed to be capable of containing one, two, three, four or even more charm quarks. Although the  $J/\psi$  meson composed of a charmanticharm pair was discovered fifty-one years ago [1, 2] and the D meson composed of a charm-antilight quark two years later [3], it was not until 2020 that the LHCb experiment found the first evidence of a pure charm tetraquark state, the X(6900), in the  $J/\psi$ -pair invariant mass spectrum—using a data sample corresponding to an integrated luminosity of  $9fb^{-1}$ —thereby providing a signal for a hadron with multiple charm quarks [4].

Using a data sample fifteen times larger but with a focus on the small rapidity region, both the ATLAS and CMS collaborations have confirmed the narrow X(6900) state and observed another narrow structure around 7100MeV and a broad structure above twice the  $J/\psi$  mass [5, 6].

Several particularly interesting aspects of these exotic states in the  $J/\psi$ -pair spectrum include: (1)the spinparity quantum numbers for all observed data distributions are found to be compatible with the  $J^{PC} = 2^{++}$ hypothesis from the very recent CMS analysis [7], which constrains the possible internal quark configuration for these exotic structures; (2) a Regge trajectory is predicted and observed from their mass spectrum [8, 9], which gives hints of a radial or orbital excitation tetraquark family; (3) examination of data from three experiments reveals that the production rate of the fully charm tetraquark state is unaffected by rapidity, yet its signal is strongly enhanced at high transverse momentum, which can be inferred that the dependence on rapidity across low to medium values should be mild, and that the transverse momentum distribution curves for  $J/\psi$ -pair and for the tetraquark state themselves should be distinct.

Addressing and clarifying the above three points requires both a consistent theoretical framework and precise calculations. From the perspective of group theory,

the fully charm tetraquark states can always be represented by a complete set of basis states. In terms of color space, one can choose either the color-symmetryantisymmetry  $\mathbf{6} \otimes \mathbf{\bar{6}}/\mathbf{\bar{3}} \otimes \mathbf{3}$  basis or the color-singlet-octet  $1 \otimes 1/8 \otimes 8$  basis. In color-symmetry-antisymmetry basis, the two charm quarks can form the "good" axial-vector diquark with antisymmetric color  $\bar{3}$  and symmetric spinflavor configuration or "bad" scalar diquark with symmetric color 6 and symmetric spin-flavor configuration. The two charm antiquarks do similarly. Both charm diquark and antidiquark carry colour charge and form a colour-charge-neutral and tightly-bound hadron from a QCD confining attractive force. Interestingly, charm diquark here is distinctly different from light-diquark system, due to the additional constraint of isospin symmetry present in the latter. In color-singlet-octet basis, the two pair of charm quark-antiquark can form a color-singlet charmonium or a color-octet cluster separately, then the two charmonia or coloured clusters form a colour-chargeneutral and loosely-bound molecule hadron from either a residual strong interaction or a repulsive force within QCD.

A true physical system may reside in one of the basis states mentioned above, or in a superposition of these basis states. For example, we can expand the fully heavy tetraquark state within the color-symmetry-antisymmetry basis as

$$|T_{4Q}\rangle = \sum_{L=0} C_L^s |(Q_1 Q_2)_0; (\bar{Q}_3 \bar{Q}_4)_0; L\rangle + C_L^a |(Q_1 Q_2)_1; (\bar{Q}_3 \bar{Q}_4)_1; L\rangle,$$
(1)

where  $C_L^s$  and  $C_L^a$  are the symmetric and antisymmetric configuration coefficients with  $\sum_{L=0} |C_L^s|^2 + |C_L^a|^2 = 1$ , respectively. Orbital excitation effects are marked with L. The higher Fock states with gluon content are omitted here but can be included in a similar manner.

In this Letter, we calculate the differential and total cross sections for the hadronic production of S-wave fully

<sup>&</sup>lt;sup>1</sup>Department of Physics and Institute of Theoretical Physics, Nanjing Normal University, Nanjing, Jiangsu 210023, China <sup>2</sup>Nanjing Key Laboratory of Particle Physics and Astrophysics, Nanjing Normal University, Nanjing, Jiangsu 210023, China

charm tetraquark states based on the color-symmetryantisymmetry basis and nonrelativisitic QCD (NRQCD) effective theory. Our calculations include contributions from all possible configurations, such as  $J^{PC} = 0^{++}$  or 2<sup>++</sup>, as well as mixing effects arising from identical quantum numbers. On hadron colliders, gluon radiation effects are non-negligible; therefore, we provide a complete treatment of QCD corrections up to the next-to-leading order (NLO). When the transverse momentum of the fully charm tetraquark state is much lower than its typical momentum scale, we perform resummation at the next-to-leading logarithmic (NLL) accuracy to mitigate large logarithmic terms induced by soft gluon emissions in the low transverse momentum region. These physical results will aid in identifying the quantum numbers and microscopic structures of fully charm tetraquark states, while also facilitating the understanding of the physical mechanisms behind the observed signal enhancement at high transverse momenta.

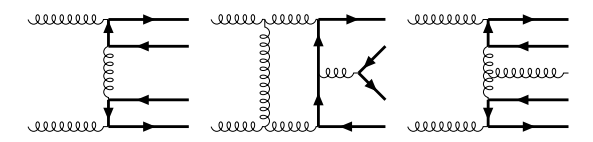


FIG. 1. Typical Feynman diagrams for the gluon-gluon fusion to fully charm tetraquark up to NLO. The thick black lines stand for the massive charm quarks. The Feynman diagrams from the quark-antiquark annihilation or (anti)quark-gluon scattering can be plotted similarly.

QCD factorization formulae. The typical Feynman diagrams for fully charm tetraquark hadronic production are plotted in Fig. 1. The hadronic production of fully charm tetraquark can be factorized as

$$\frac{d\sigma}{dydP_{\perp}^{2}}(p+p\to T_{4c}+X) 
= \sum_{i} \int_{x_{A}}^{1} d\xi_{1} f_{i/A}(\xi_{1},\mu_{F}) \sum_{j} \int_{x_{B}}^{1} d\xi_{2} f_{j/B}(\xi_{2},\mu_{F}) 
\times \int d^{2}b e^{iP_{\perp}\cdot b} W(b,\xi_{1},\xi_{2},M) \hat{\sigma}_{ij}^{(0)} C_{iA} \left(\frac{x_{A}}{\xi_{1}},\alpha_{s}(\mu_{F})\right) 
\times C_{jB} \left(\frac{x_{B}}{\xi_{2}},\alpha_{s}(\mu_{F})\right) + Y(P_{\perp},M,x_{A},x_{B}), \tag{2}$$

where y and  $P_{\perp}$  are the rapidity and transverse momentum for fully charm tetraquark.  $f_{i/A}$  and  $f_{j/B}$  are parton distribution functions of parton in the proton.  $W(b,\xi_1,\xi_2,M)$  is the Fourier transformation of the differential cross section at low  $P_{\perp}$  into the impact parameter b-space considering the resummation contribution.  $C_{iA}$  and  $C_{jB}$  are the matching coefficients.  $Y(P_{\perp},M,x_A,x_B)$  is the regular term contributing the medium and large  $P_{\perp}$  region.

In the factorization formuale,  $\hat{\sigma}_{ij}^{(0)}$  is related to the

leading-order (LO) partonic cross section  $\hat{\sigma}^{(LO)}(i+j \to T_{4c}) = \hat{\sigma}^{(0)}_{ij} \delta(1-z)$  with  $z = M^2/\hat{s}$  where M is the fully charm tetraquark mass and  $\hat{s}$  is the center-of-mass energy in partonic frame. We have

$$\hat{\sigma}_{ij}^{(0)} = \frac{\pi}{M^4} \frac{1}{c_i c_j s_i s_j} \left| \mathcal{M}_{ij}^{(0)} \right|^2, \tag{3}$$

where the color and spin average factor are  $c_g=N_c^2-1$ ,  $c_q=f_{\bar q}=N_c$ ,  $s_g=2-2\epsilon$ , and  $s_q=s_{\bar q}=2$ . The Feynman amplitude squared from certain operator contribution can be written as

$$\left| \mathcal{M}_{ij}^{(n)} \right|_{O_{g_1,g_2}^J}^2 = \frac{M\pi^4 \alpha_s^4}{128m_c^8} c_{ij,O_{g_1,g_2}}^{(n)} \langle 0|O_{g_1,g_2}^J|0\rangle. \tag{4}$$

In this expression,  $m_c$  is the charm quark mass.  $O_{g_1,g_2}^J$  are the NRQCD long-distance operators for tetraquarks with spin quantum number J

$$O_{g_1,g_2}^J = \mathcal{O}_{g_1}^{(J)} \sum_{X} |T_{4c}^J + X\rangle \langle T_{4c}^J + X| \mathcal{O}_{g_2}^{(J)\dagger}.$$
 (5)

Therein  $g_i$  can be either  $\mathbf{6} \otimes \overline{\mathbf{6}}$  or  $\overline{\mathbf{3}} \otimes \mathbf{3}$  in color symmetry-antisymmetry basis. Then we have [10, 11]

$$\mathcal{O}_{\overline{\mathbf{3}}\otimes\mathbf{3}}^{(0)} = -\frac{1}{\sqrt{3}} \left[ \psi_a^T \left( i\sigma^2 \right) \sigma^i \psi_b \right] \left[ \chi_c^{\dagger} \sigma^i \left( i\sigma^2 \right) \chi_d^* \right] \mathcal{C}_{\overline{\mathbf{3}}\otimes\mathbf{3}}^{ab;cd},$$

$$\mathcal{O}_{\overline{\mathbf{3}}\otimes\mathbf{3}}^{(2;ij)} = \left[ \psi_a^T \left( i\sigma^2 \right) \sigma^m \psi_b \right] \left[ \chi_c^{\dagger} \sigma^n \left( i\sigma^2 \right) \chi_d^* \right] \Gamma^{ij;mn} \mathcal{C}_{\overline{\mathbf{3}}\otimes\mathbf{3}}^{ab;cd},$$

$$\mathcal{O}_{\overline{\mathbf{6}}\otimes\overline{\mathbf{6}}}^{(0)} = \left[ \psi_a^T \left( i\sigma^2 \right) \psi_b \right] \left[ \chi_c^{\dagger} \left( i\sigma^2 \right) \chi_d^* \right] \mathcal{C}_{\overline{\mathbf{6}}\otimes\overline{\mathbf{6}}}^{ab;cd}, \tag{6}$$

where the rank-4 color tensor is defined as  $C_{\mathbf{6}\otimes\mathbf{6}}^{cd;ef} = \frac{1}{2\sqrt{6}} \left( \delta_{ce} \delta_{df} + \delta_{cf} \delta_{de} \right)$  and  $C_{\mathbf{3}\otimes\mathbf{3}}^{cd;ef} = \frac{1}{2\sqrt{3}} \left( \delta_{ce} \delta_{df} - \delta_{cf} \delta_{de} \right)$ . The rank-4 Lorentz tensor is defined as  $\Gamma^{\alpha\beta;\mu\nu} = \frac{1}{2} g^{\mu\alpha} g^{\nu\beta} + \frac{1}{2} g^{\mu\beta} g^{\nu\alpha} - \frac{1}{3} g^{\mu\nu} g^{\alpha\beta}$ .

At LO, the short-distance coefficients for gluon-gluon fusion are

$$c_{gg,O_{g_1,g_2}}^{(0)} = \{\frac{15488}{27}, 2304, \frac{1408\sqrt{6}}{3}, \frac{200704}{27}\}, \quad (7)$$

for  $O_{g_1,g_2}^J=O_{\mathbf{6}\otimes\overline{\mathbf{6}},\mathbf{6}\otimes\overline{\mathbf{6}}}^0,O_{\overline{\mathbf{3}}\otimes\mathbf{3},\overline{\mathbf{3}}\otimes\mathbf{3}}^0,O_{\mathbf{6}\otimes\overline{\mathbf{6}},\overline{\mathbf{3}}\otimes\mathbf{3}}^0,O_{\overline{\mathbf{3}}\otimes\mathbf{3},\overline{\mathbf{3}}\otimes\mathbf{3}}^2,$  respectively. The result for  $O_{\overline{\mathbf{3}}\otimes\mathbf{3},\mathbf{6}\otimes\overline{\mathbf{6}}}^0$  is the same as for  $O_{\mathbf{6}\otimes\overline{\mathbf{6}},\overline{\mathbf{3}}\otimes\mathbf{3}}^0$ . We observe that the non-valishing contribution in quark-antiquark annihilation at LO is for spin-2 tetaquark with  $c_{q\bar{q},O_{\overline{\mathbf{3}}\otimes\mathbf{3},\overline{\mathbf{3}}\otimes\mathbf{3}}^{(0)}=32768/9$ .

At LO, there are 62 and 4 tree-level non-vanishing Feynman diagrams contributing to  $g+g \to T_{4c}$  and  $q+\bar{q}\to T_{4c}$ . Since it is a 2-to-4-body process at the partonic level, this process can generate quite a few topological diagrams. At NLO, there are 2008 and 170 one-loop non-vanishing Feynman diagrams contributing to  $g+g\to T_{4c}$  and  $q+\bar{q}\to T_{4c}$ . Also we need to consider the real corrections and find 618, 98 and 98 tree-level non-vanishing Feynman diagrams contributing to

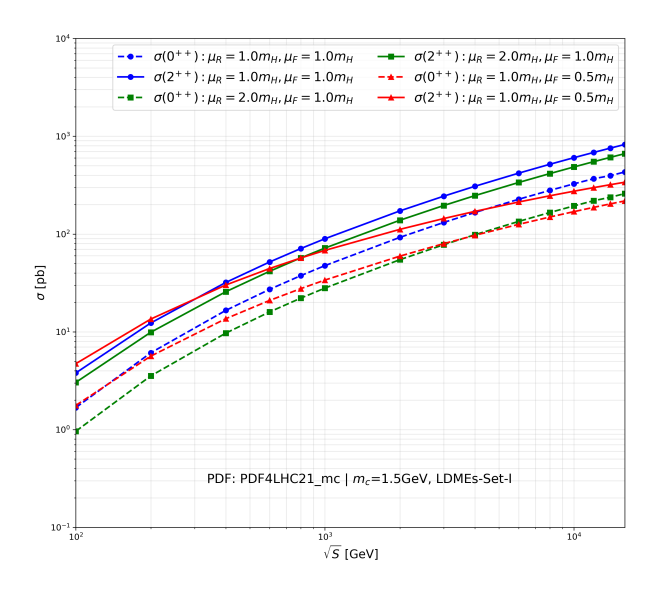


FIG. 2. NLO cross-section results for the fully charm tetraquark dependence on the hadron-hadron center-of-mass energy  $\sqrt{S}$ . X(6900) is assumed to be  $2^{++}$  and its  $0^{++}$  partner is also plotted. The comparison with three choices of renormalization and factorization scales are given.

 $g+g \to T_{4c}+g, \ q+\bar{q} \to T_{4c}+g$  and  $q+g \to T_{4c}+q$ , respectively. Dimensional regularization with  $D=4-2\epsilon$  is employed for both UV and IR divergences.

We have generated the tree-level and one-loop amplitude by using the package FeynArts [12]. After substituting the fermion chains, the package FeynCalc [13, 14] is used to simplify the Dirac matrices. Then the amplitudes can be expressed by the several form factor,

$$\mathcal{M}_{ij}^{(1)} = \sum_{k=1}^{10} d_k F_k. \tag{8}$$

Then the corresponding coefficients  $\{d_k\}$  are the linear combinations of one-loop scalar integrals, which can be reduced to a set of basis integrals called master integrals (MIs) due to the identities from integration by parts (IBP) [15, 16] with the package Kira [17]. The analytical results of one-loop MIs can be easily obtained by package FeynHelpers [18] based on Package-X [19]. In addition, the ward identity is used to check our result.

The NLO virtual correction to the partonic crosssection can be expressed by

$$2|\mathcal{M}_{ij}^{(0)}\mathcal{M}_{ij}^{(1)\dagger}| = |\mathcal{M}_{ij}^{(0)}|^2 \left(\frac{\alpha_s}{\pi}\right) \Gamma(1+\epsilon) (4\pi)^{\epsilon} K_{ij}^{V}.$$
 (9)

As a concrete demonstration, the analytic expression for the  $2^{++}$  tetraquark from gluon-gluon fusion reads

$$K_{gg,\overline{\mathbf{3}}\otimes\mathbf{3}}^{\mathrm{V},2++} = \frac{3}{\epsilon^2} - \frac{1}{\epsilon} \left( 3\log\left(\frac{\mu_R^2}{16m_c^2}\right) - \frac{n_l}{3} + \frac{11}{2} \right) - \frac{3}{2}\log^2\left(\frac{\mu_R^2}{16m_c^2}\right) + \left(\frac{11}{2} - \frac{2n_h + n_l}{3}\right) \log\left(\frac{\mu_R^2}{m_c^2}\right) \\ - \frac{31603}{2016} \mathrm{Li}_2\left(\frac{1}{3}\right) - \frac{155}{504} \mathrm{Li}_2\left(-\frac{1}{3}\right) + \frac{3(11 + n_h)}{112} \log^2\left(7 - 4\sqrt{3}\right) - \frac{(1109 - 19n_h)}{112} \log^2\left(2\sqrt{2} + 3\right) \\ + \frac{\pi^2(-14251 + 720n_h)}{8064} - \frac{10741}{1344} \log^2(3) - \frac{11 + 3n_h}{2\sqrt{3}} \log\left(4\sqrt{3} + 7\right) + \frac{(2027 + 6n_h)}{42\sqrt{2}} \log\left(2\sqrt{2} + 3\right) \\ + \frac{(97655 - 3888n_l)}{4536} \log(2) + \frac{611 - 1740n_h - 912n_l}{1512} + \mathcal{O}(\epsilon), \tag{10}$$

where the  $n_l(n_h)$  are the number of the light (heavy) quarks and  $\mu_R$  is the renormalization scale.

The NLO real correction including the gluon radiation to the partonic cross-section can be written as

$$\hat{\sigma}^{\text{NLO,R}} (i+j \to T_{4c} + k) = \frac{1}{2\hat{s}} \frac{4^{\epsilon}}{\Gamma(1-\epsilon)} \left( \frac{4\pi\mu_R^2}{\hat{s}} \right)^{\epsilon} \frac{1}{16\pi} (1-z)^{1-2\epsilon} \times \int_{-1}^{1} dy_{\theta} \left( 1 - y_{\theta}^2 \right)^{-\epsilon} \frac{1}{c_i c_j s_i s_j} \left| \mathcal{M}_{ijk}^{(1)} \right|^2 (z, y_{\theta}), \quad (11)$$

where  $y_{\theta} = \cos \theta$  with the angle  $\theta$  between the momenta of initial parton i and the tetraquark in lab frame. The

explicit expressions for  $\left|\mathcal{M}_{ijk}^{(1)}\right|^2$  and the virtual correction  $K_{ij}^{\mathrm{V}}$  are listed in the Supplemental material.

The soft IR divergences are cancelled between virtual and real corrections, while the residual IR divergences can be cancelled by the renormalization of parton distribution functions. We find that the renormalization constants of the color singlet four charm quark operators in Eq. (6) are exactly unity at the order of  $\mathcal{O}(\alpha_s)$ , which has never been explored in prior works.

Constraints on long-distance operator matrix elements for fully charm tetraquark. The aforementioned factorization formula is generally regarded as a modelindependent effective theory derived from QCD, which factorizes the short-distance hard scattering processes from the non-perturbative interactions desribed by the long-distance matrix elements (LDMEs). The LDMEs are process-independent input parameters. There are four LDMEs for fully charm tetraquark in this work. We rewrite them as

$$\langle \mathcal{O}_{6\overline{6}}^{T4c} \rangle \left( {}^{1}S_{0} \right) = \langle 0|O_{\mathbf{6}\otimes\overline{\mathbf{6}},\mathbf{6}\otimes\overline{\mathbf{6}}}^{0}|0\rangle, 
\langle \mathcal{O}_{3\overline{3}}^{T4c} \rangle \left( {}^{1}S_{0} \right) = \langle 0|O_{\mathbf{3}\otimes\mathbf{3},\overline{\mathbf{3}}\otimes\mathbf{3}}^{0}|0\rangle, 
\langle \mathcal{O}_{mix}^{T4c} \rangle \left( {}^{1}S_{0} \right) = \langle 0|O_{\mathbf{6}\otimes\overline{\mathbf{6}},\overline{\mathbf{3}}\otimes\mathbf{3}}^{0}|0\rangle,$$
(12)

for  $0^{++}$  fully charm tetraquark, and

$$\langle \mathcal{O}_{3\bar{3}}^{T4c} \rangle \left( {}^{5}S_{2} \right) = \langle 0|O_{\overline{3} \otimes 3\overline{3} \otimes 3}^{2}|0\rangle,$$
 (13)

for  $2^{++}$  fully charm tetraquark.

In LHCb experiment, the production cross-section of the X(6900) structure relative to that of  $J/\psi$ -pair, times the branching fraction  $\mathcal{B}(X(6900) \to J/\psi + J/\psi)$  is measured to be  $\mathcal{R} = [1.1 \pm 0.4(stat) \pm 0.3(syst)]\%$  in the proton-proton collision data at  $\sqrt{S} = 13TeV$  [4]. The prompt cross-section of  $J/\psi$ -pair at the same center-of-mass energy has also been measured to be  $16.36 \pm 0.28(stat) \pm 0.88(syst)nb$  in the transverse momentum range  $0 < P_{\perp} < 14GeV$  and the rapidity range 2.0 < y < 4.5 [20]. Considering the cross-section of  $J/\psi$ -pair in all  $P_{\perp}$  and y range, there is a factor around 4 to 4.8 from the theoretical calculation [21]. Thus the total cross-section of the X(6900) at  $\sqrt{S} = 13TeV$  can be estimated taking the biggest uncertainty into account

$$\sigma(X(6900))\mathcal{B}(X(6900) \to J/\psi + J/\psi) = 0.72^{+0.79}_{-0.48}nb.$$
 (14)

Assuming the X(6900) is a  $2^{++}$  tetraquark from the observation from CMS experiment [7] and its  $J/\psi$ -pair decay branching ratio around 1, we plot the NLO cross-section results for the fully charm tetraquark for various center-of-mass energy. In numerical calculation, the PDF4LHC21 combination of global PDF fits for the LHC Run III is employed [22, 23]. The mass of X(6900) is setted the newly value 6847MeV. The  $2^{++}$  LDMEs is then determined as  $\langle \mathcal{O}_{33}^{T4c} \rangle$  ( $^5S_2$ ) =  $6.16 \times 10^{-5} GeV^9$ . The ratio among various LDMEs are also considered, i.e.  $\langle \mathcal{O}_{66}^{T4c} \rangle$  ( $^1S_0$ ) :  $\langle \mathcal{O}_{33}^{T4c} \rangle$  ( $^1S_0$ ) :  $\langle \mathcal{O}_{mix}^{T4c} \rangle$  ( $^1S_0$ ) :  $\langle \mathcal{O}_{mix}^{T4c} \rangle$  ( $^1S_0$ ) :  $\langle \mathcal{O}_{mix}^{T4c} \rangle$  ( $^1S_0$ ) is equal to [1, 2.7, 1.6, 5.6] (Set-I) and [1, 1.3, -1.2, 4.5](Set-II) [11, 24–26]. By calculation, we find that the NLO K factor for the cross section at 13TeV is 2.31 and 1.09 for the  $0^{++}$  and  $2^{++}$  configuration, respectively. Both the NLO K factors increase when the center-of-mass energy decreases.

Discussions and conclusion

We also plot the rapidity and transverse momentum distribution in Figs 3 and 4 for different quark configurations. The differential cross section exhibits a relatively flat profile in rapidity, particularly across the low

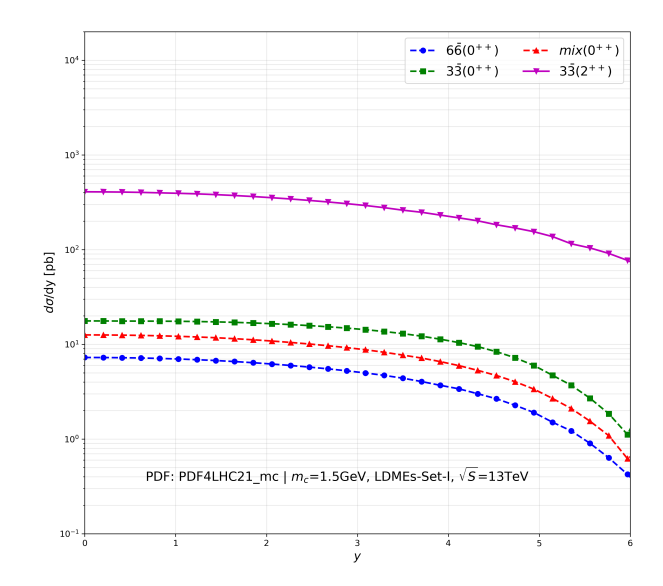


FIG. 3. NLO differential cross-sections for the fully charm tetraquark with different quark configurations dependence on the rapidity y.

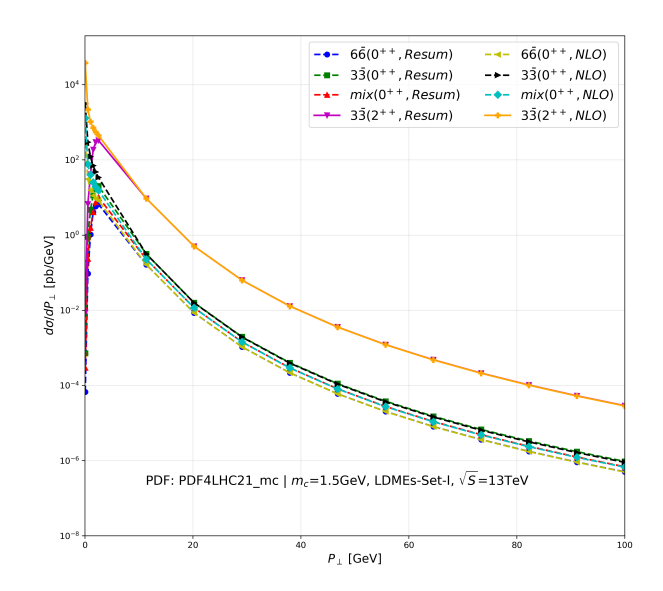


FIG. 4. NLO and Resum (NLO after resummation) differential cross-sections for the fully charm tetra quark with different quark configurations dependence on the transverse momentum  $P_{\perp}.$ 

and intermediate rapidity ranges. The contribution from the  $2^{++}$  configuration is significantly enhanced—for instance, it is nearly two orders of magnitude higher than that of the  $6\bar{6}(0^{++})$  configuration. This enhancement stems not only from differences in LDMEs, but also

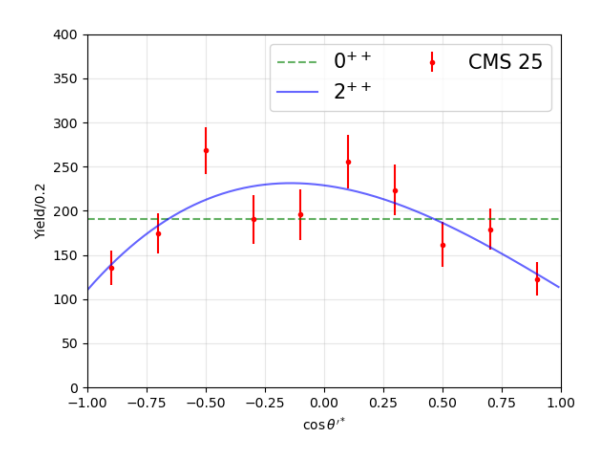


FIG. 5. Distribution of the polar angle  $\theta'^*$  between the  $J/\psi$  and the fully charm tetraquark momenta. The CMS 25 data is from the very recent measurement by the CMS experiment [7].

from the difference in short-distance coefficients, a finding which is also consistent with previous theoretical and experimental works [7, 8, 27–31].

In NLO calculations, UV and IR divergences arise from loop diagrams and real corrections. The UV divergences can be rigorously canceled through the renormalization procedure, while the soft IR divergences cancel between the loop and real correction terms, leaving only the collinear divergences. The divergence-free pattern is also first observed in the quadripole picture of fully charm tetraquark, then we do not need introduce any NRQCD operator renormalization here. The final collinear divergences are obsorbed into the parton distribution functions.

The effects of soft and collinear gluon radiation induce singular structures, specifically terms proportional to  $1/P_{\perp}$  and  $\ln(P_{\perp}^2/M^2)/P_{\perp}$ , in the transverse momentum distribution. This undermines the reliability of the theoretical prediction at low  $P_{\perp}$ . By the standard resummation procedure, these singularities at the Fourier transformation impact parameter b-space will be canceled between the loop and real correction terms while the large logrithems can be resummed at NLL accuracy [32, 33]. We also show the resummation results for the transverse momentum distribution in Fig 4. We observe that the transverse momentum distribution is steeper than the rapidity distribution. However, it is flatter than the  $J/\psi$ -pair transverse momentum distribution, particularly at  $0 < P_{\perp} < 20 GeV$ . This relative flatness can explain the LHCb data with X(6900) signal enhancement at high transverse momenta.

Furthermore we consider the two-body decays of fully charm tetraquarks where the  $0^{++}$  state will only produce an isotropic polar angular distribution, while the distribution for the  $2^{++}$  state will be non-trivial. We

can always expand the polar angular distribution of the produced  $2^{++}$  fully charm tetraquark state into  $J/\psi$  pair as  $dN/d\cos\theta'^* = \sum_{i=1}^4 L_i \cos[(i-1)\theta'^*]$ , where the coefficients  $L_i$  depend on the production and decay mechanisms and  $\theta'^*$  is the polar angle between one of  $J/\psi$  and the fully charm tetraquark momenta. Fortunately, the CMS experiment has measured the polar angular distribution with  $135fb^{-1}$ , allowing us to fit these parameters. We show the results in Fig 5, the parameters for  $2^{++}$  have been fitted as  $L_1 = 170.0(7.9)$ ,  $L_2 = -8(13)$ ,  $L_3 = -59(12), L_4 = 9(13)$  with  $\chi^2/dof = 1.8$ , which determine the correlation between the production and decay of the fully charm tetraquark state. Due to the complexity of the CMS analysis where all the three peaks are included, we defer a detailed discussion to future work. The polar angle  $\theta'^*$  distribution from the CMS experiment support the  $J^{PC} = 2^{++}$  assignment for the exotic structures in the  $J/\psi$  pair final states.

We would like to conclude this work with the following remarks. First, our theoretical framework is built upon the fundamental principles of QCD and systematic symmetry analysis, ensuring the rigor of both the theoretical framework and the analytical results. Second, by utilizing LHCb and CMS experimental data, we have for the first time constrained and extracted the non-perturbative LDMEs for X(6900). These results can be widely applied to other reaction processes involving X(6900). Third, while the current discussion is limited to S-wave states without orbital excitation, even if contributions from P-wave [34] or higher partial waves need to be considered in the future, the S-wave results presented in this work should remain essential and critical for understanding these exotic hadrons. This is because we believe the basis expansion method based on symmetry is effective and covers these exotic states with corresponding coefficients. With the increasing data samples collected by the LHC, we also hope that experimental colleagues will perform more precise measurements of (differential) cross sections, rapidity and transverse momentum distributions for exotic hadrons in  $J/\psi$ -pair mass spectrum. Such efforts will provide further insights into clarifying the structural properties of these states, particularly regarding the existence of compact clustering mechanisms.

Acknowledgments. Thanks to Prof. Liu-Pan An, Prof. Zhi-Guo He and Mr. Kaiwen Chen for useful discussions. This work is supported by the National Natural Science Foundation of China Grants No.12322503, No.12405117 and No.12075124.

<sup>\*</sup> wangyefan@nnu.edu.cn

<sup>†</sup> rlzhu@njnu.edu.cn

 <sup>[1]</sup> J. J. Aubert et al. [E598], Phys. Rev. Lett. 33, 1404-1406
 (1974) doi:10.1103/PhysRevLett.33.1404

<sup>[2]</sup> J. E. Augustin et al. [SLAC-SP-017], Phys. Rev. Lett.

- **33**, 1406-1408 (1974) doi:10.1103/PhysRevLett.33.1406
- [3] G. Goldhaber, F. Pierre, G. S. Abrams, M. S. Alam, A. Boyarski, M. Breidenbach, W. C. Carithers, W. Chinowsky, S. Cooper and R. DeVoe, et al. Phys. Rev. Lett. 37, 255-259 (1976) doi:10.1103/PhysRevLett.37.255
- [4] R. Aaij et al. [LHCb], Sci. Bull. 65, no.23, 1983-1993 (2020) doi:10.1016/j.scib.2020.08.032 [arXiv:2006.16957 [hep-ex]].
- [5] G. Aad et al. [ATLAS], Phys. Rev. Lett. 131, no.15, 151902 (2023) doi:10.1103/PhysRevLett.131.151902
   [arXiv:2304.08962 [hep-ex]].
- [6] A. Hayrapetyan et al. [CMS], Phys. Rev. Lett. 132, no.11, 111901 (2024) doi:10.1103/PhysRevLett.132.111901 [arXiv:2306.07164 [hep-ex]].
- [7] A. Hayrapetyan *et al.* [CMS], [arXiv:2506.07944 [hep-ex]].
- [8] R. Zhu, Nucl. Phys. B 966, 115393 (2021) doi:10.1016/j.nuclphysb.2021.115393 [arXiv:2010.09082 [hep-ph]].
- [9] F. Zhu, G. Bauer and K. Yi, Chin. Phys. Lett. 41, no.11, 111201 (2024) doi:10.1088/0256-307X/41/11/111201 [arXiv:2410.11210 [hep-ph]].
- [10] G. T. Bodwin, E. Braaten and G. P. Lepage, Phys. Rev. D 51, 1125-1171 (1995) [erratum: Phys. Rev. D 55, 5853 (1997)] doi:10.1103/PhysRevD.55.5853 [arXiv:hep-ph/9407339 [hep-ph]].
- [11] F. Feng, Y. Huang, Y. Jia, W. L. Sang, D. S. Yang and J. Y. Zhang, Phys. Rev. D 108, no.5, L051501 (2023) doi:10.1103/PhysRevD.108.L051501 [arXiv:2304.11142 [hep-ph]].
- [12] T. Hahn, Comput. Phys. Commun. 140, 418-431
   (2001) doi:10.1016/S0010-4655(01)00290-9 [arXiv:hep-ph/0012260 [hep-ph]].
- [13] V. Shtabovenko, R. Mertig and F. Orellana, Comput. Phys. Commun. 256, 107478 (2020) doi:10.1016/j.cpc.2020.107478 [arXiv:2001.04407 [hep-ph]].
- [14] V. Shtabovenko, R. Mertig and F. Orellana, Comput. Phys. Commun. 306, 109357 (2025) doi:10.1016/j.cpc.2024.109357 [arXiv:2312.14089 [hep-ph]].
- [15] F. V. Tkachov, Phys. Lett. B 100, 65-68 (1981) doi:10.1016/0370-2693(81)90288-4
- [16] K. G. Chetyrkin and F. V. Tkachov, Nucl. Phys. B 192, 159-204 (1981) doi:10.1016/0550-3213(81)90199-1
- [17] J. Klappert, F. Lange, P. Maierhöfer and J. Usovitsch, Comput. Phys. Commun. 266, 108024 (2021) doi:10.1016/j.cpc.2021.108024 [arXiv:2008.06494 [hep-ph]].
- [18] V. Shtabovenko, Comput. Phys. Commun. 218, 48-65

- $\begin{array}{lll} (2017) & doi:10.1016/j.cpc.2017.04.014 & [arXiv:1611.06793 \\ [physics.comp-ph]]. \end{array}$
- [19] H. H. Patel, Comput. Phys. Commun. 197, 276-290 (2015) doi:10.1016/j.cpc.2015.08.017 [arXiv:1503.01469 [hep-ph]].
- [20] R. Aaij et al. [LHCb], JHEP 03, 088 (2024) doi:10.1007/JHEP03(2024)088 [arXiv:2311.14085 [hep-ex]].
- [21] Z. G. He, X. B. Jin and B. A. Kniehl, Phys. Rev. D 111, no.9, 094040 (2025) doi:10.1103/PhysRevD.111.094040 [arXiv:2505.04357 [hep-ph]].
- [22] R. D. Ball et al. [PDF4LHC Working Group], J. Phys. G 49, no.8, 080501 (2022) doi:10.1088/1361-6471/ac7216 [arXiv:2203.05506 [hep-ph]].
- [23] A. Buckley, J. Ferrando, S. Lloyd, K. Nordström, B. Page, M. Rüfenacht, M. Schönherr and G. Watt, Eur. Phys. J. C 75, 132 (2015) doi:10.1140/epjc/s10052-015-3318-8 [arXiv:1412.7420 [hep-ph]].
- [24] W. L. Sang, T. Wang, Y. D. Zhang and F. Feng, Phys. Rev. D **109**, no.5, 056016 (2024) doi:10.1103/PhysRevD.109.056016 [arXiv:2307.16150 [hep-ph]].
- [25] Q. F. Lü, D. Y. Chen and Y. B. Dong, Eur. Phys. J. C 80, no.9, 871 (2020) doi:10.1140/epjc/s10052-020-08454-1 [arXiv:2006.14445 [hep-ph]].
- [26] M. S. liu, F. X. Liu, X. H. Zhong and Q. Zhao, Phys. Rev. D 109, no.7, 076017 (2024) doi:10.1103/PhysRevD.109.076017 [arXiv:2006.11952 [hep-ph]].
- [27] K. Chen, F. X. Liu, Q. Zhao, X. H. Zhong, R. Zhu and B. S. Zou, [arXiv:2412.13455 [hep-ph]].
- [28] F. G. Celiberto, [arXiv:2507.09744 [hep-ph]].
- [29] H. F. Zhang, Y. Q. Ma and W. L. Sang, Sci. Bull. 70, 1915-1917 (2025) doi:10.1016/j.scib.2025.04.035 [arXiv:2009.08376 [hep-ph]].
- [30] F. Feng, Y. Huang, Y. Jia, W. L. Sang, X. Xiong and J. Y. Zhang, Phys. Rev. D 106, no.11, 114029 (2022) doi:10.1103/PhysRevD.106.114029 [arXiv:2009.08450 [hep-ph]].
- [31] I. Belov, A. Giachino and E. Santopinto, JHEP 01, 093 (2025) doi:10.1007/JHEP01(2025)093 [arXiv:2409.12070 [hep-ph]].
- [32] J. C. Collins, D. E. Soper and G. F. Sterman, Nucl. Phys. B 250, 199-224 (1985) doi:10.1016/0550-3213(85)90479-1
- [33] H. X. Zhu, C. S. Li, H. T. Li, D. Y. Shao and L. L. Yang, Phys. Rev. Lett. 110, no.8, 082001 (2013) doi:10.1103/PhysRevLett.110.082001 [arXiv:1208.5774 [hep-ph]].
- [34] W. L. Wu, Y. K. Chen, L. Meng and S. L. Zhu, Phys. Rev. D 109, no.5, 054034 (2024) doi:10.1103/PhysRevD.109.054034 [arXiv:2401.14899 [hep-ph]].